

# Highly efficient single-longitudinal-mode $\beta$ -BaB<sub>2</sub>O<sub>4</sub> optical parametric oscillator with a new cavity design

**J. M. Boon-Engering**

*Nederlands Centrum voor Laser Research b.v., Postbus 2662, 7500 CR Enschede, The Netherlands, and  
Department of Physics and Astronomy, Laser Centre Vrije Universiteit, De Boelelaan 1081, 1081 HV Amsterdam, The Netherlands*

**L. A. W. Gloster**

*Laser Photonics Group, Department of Physics and Astronomy, University of Manchester, Manchester M13 9PL, UK*

**W. E. van der Veer**

*Nederlands Centrum voor Laser Research b.v., Postbus 2662, 7500 CR Enschede, The Netherlands, and  
Department of Physics and Astronomy, Laser Centre Vrije Universiteit, De Boelelaan 1081, 1081 HV Amsterdam, The Netherlands*

**I. T. McKinnie**

*Laser Photonics Group, Department of Physics and Astronomy, University of Manchester, Manchester M13 9PL, UK, and  
Department of Physics, University of Otago, P.O. Box 56, Dunedin, New Zealand*

**T. A. King**

*Laser Photonics Group, Department of Physics and Astronomy, University of Manchester, Manchester M13 9PL, UK*

**W. Hogervorst**

*Department of Physics and Astronomy, Laser Centre Vrije Universiteit, De Boelelaan 1081, 1081 HV Amsterdam, The Netherlands*

Received June 8, 1995

A new coupled-cavity design for single-longitudinal-mode operation of an optical parametric oscillator (OPO) is presented. The OPO is based on a  $\beta$ -BaB<sub>2</sub>O<sub>4</sub> crystal and is pumped by the third harmonic of a Nd:YAG laser. With this design, we achieved single-longitudinal-mode operation of the OPO with a decrease in the threshold and an increase in external efficiency compared with those of a conventional grazing-incidence OPO. A mathematical model that describes the mode spacings for this cavity is given. © 1995 Optical Society of America

Optical parametric oscillators (OPO's) are attractive solid-state sources of coherent radiation with extensive tuning ranges and high efficiencies.<sup>1</sup> However, free-running OPO's exhibit a broad spectral bandwidth that is not desirable for many applications. Several mechanisms have been explored to produce a narrow linewidth: injection seeding with a narrow-band laser<sup>2</sup> and the use of frequency-selective intracavity elements such as étalons.<sup>3</sup> Another technique to reduce the spectral bandwidth is to use a cavity in a grazing-incidence configuration.<sup>4</sup> For an OPO based on KTP in this configuration, single-longitudinal-mode (SLM) operation has been achieved.<sup>4</sup> This configuration has also been used to minimize the bandwidth of an OPO based on  $\beta$ -BaB<sub>2</sub>O<sub>4</sub> (BBO), as we reported recently.<sup>5</sup> However, the external efficiency of such a cavity was low, and we found stable SLM operation difficult to achieve.

In this Letter we present an OPO with a new cavity design based on the grazing-incidence configuration. The new design includes an additional mirror that couples back a small part of the zero-order output of the cavity. We have observed reliable SLM operation of this OPO at significantly higher external efficiencies. It involves two coupled cavities: a

grazing-incidence cavity and a cavity formed by the back mirror and a zero-order mirror placed in the zero-order beam reflected from the grating. This second cavity is referred to as the linear cavity in the text. This composite resonator can be described as a Michelson-mirror cavity<sup>6</sup> with the conventional beam splitter replaced by a grating. Michelson-mirror cavities have been used to reduce the bandwidth of lasers, as reviewed by Smith.<sup>7</sup> Using a mathematical model based on the description by Smith,<sup>8</sup> we are able to calculate the mode spacing of the coupled cavity accurately. Pinard and Young investigated a Fox-Smith-type coupled cavity for an OPO.<sup>9</sup> This coupled cavity, in which the gain medium is active in only one of the two cavities, differs from that in the Michelson case, in which the gain medium is active in both cavities.<sup>7</sup>

A schematic diagram of the coupled cavity is shown in Fig. 1. It consists of a BBO crystal cut for type I phase matching ( $e \rightarrow o + o$ ) with dimensions 4 mm  $\times$  6 mm  $\times$  14 mm. The back mirror is mounted as close to the BBO crystal as possible and has a high reflectivity in the range of 630 nm  $\pm$  10%, with high transmission at the pump wavelength of 355 nm. A 1800-line/mm holographic grating

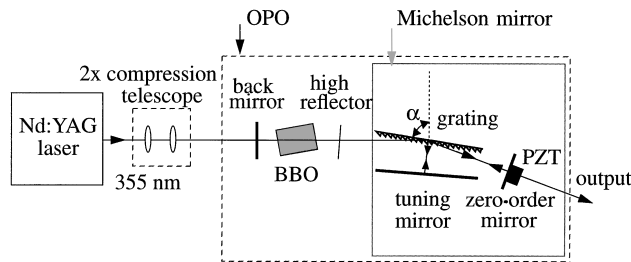


Fig. 1. Schematic diagram of the OPO. The OPO is pumped with 355-nm light from a Nd:YAG laser. Its beam size is reduced by a factor of 2 by a telescope. The Michelson-mirror part of the cavity is shown. The grating angle  $\alpha$  is indicated.

(National Physical Laboratories, UK) is positioned at grazing incidence with respect to the cavity axis. A high reflector at 355 nm is placed between the crystal and the grating to prevent residual pump light from damaging the grating surface. This reflector is placed at an angle such that the reflected pump beam is not pumping the OPO. The angle of incidence on the grating ( $\alpha$ ) is indicated in the figure and subtends the grating surface and the (dashed) line perpendicular to the resonant axis. The tuning mirror (reflectivity  $98 \pm 2\%$  for the wavelength range 500–710 nm) is mounted on a rotation stage. The pivot point coincides with the center of the crystal. It reflects first-order light from the grating back into the cavity and allows for wavelength tuning. These components make up the conventional grazing-incidence cavity. An additional mirror, positioned to couple back a proportion of the cavity output, is mounted on a piezoelectric transducer (PZT) normal to the zero-order cavity output. It has a reflectivity of  $4 \pm 0.5\%$  at the resonant signal wavelength in the wavelength range 400–710 nm. The coupled cavity is pumped at 355 nm with a 10-Hz repetition-rate, 6-ns pulse-duration injection-seeded Nd:YAG laser with a single-axial-mode linewidth of 90 MHz (Spectra-Physics GCR-4). A telescope was used to reduce the beam diameter of the pump laser by a factor of 2 to 2.5 mm ( $1/e^2$  value). The OPO was tunable from 580 to 690 nm, a range limited by the reflectivity of the back mirror.

The signal bandwidth of the OPO was investigated with a pulsed laser spectrum analyzer (Burleigh Model WA-3500), which consists of two étalons, A and B. Étalon A has a free spectral range of  $\sim 250$  GHz and a resolution of  $\sim 3$  GHz, whereas étalon B has a free spectral range of  $\sim 10$  GHz and a resolution of  $\sim 200$  MHz. We measured single-shot spectra by analyzing the étalon fringe pattern using a CCD array.

For a grating angle of  $88.6^\circ$ , the OPO was found to operate in a SLM with a bandwidth of  $210 \pm 70$  MHz at a wavelength of 610 nm, as shown in Fig. 2. The pulse duration of the OPO was  $\sim 3$  ns. The OPO could be tuned to any desired wavelength in the range 580–690 nm by adjustment of the angle of the crystal and the tuning mirror, followed by fine tuning of the cavity lengths for SLM operation. The OPO remained SLM for several minutes without any cavity adjustment. Using the PZT (maximum  $3\text{-}\mu\text{m}$  excursion) on the zero-order mirror, we adjusted the length of the linear cavity to maintain SLM operation. For stable SLM operation

the length of the linear cavity had to be adjusted within  $1/10$  of the signal wavelength.

Without the constraints imposed on the cavity by the zero-order mirror, the OPO operated at all times on two cavity modes. With the zero-order mirror in position, the external efficiency of the device increased dramatically and the operational threshold decreased as a result of the additional coupling. A threshold of 32 mJ ( $109 \text{ MW/cm}^2$ ) was recorded without the zero-order mirror, which fell to 25.5 mJ ( $87 \text{ MW/cm}^2$ ) when this mirror was introduced. The OPO output increased from 0.07 to 0.5 mJ at a pump power of 39 mJ ( $132 \text{ MW/cm}^2$ ) and shows an improved intensity stability. The slope efficiency of the OPO increased from 1% to 3.7%. Pumping at higher powers damaged the coating of the back mirror.

The mode structure of the generated radiation is sensitive to the reflectivity of the zero-order mirror. For the Michelson-mirror cavity to be frequency selective its value must be similar to the grating diffraction efficiency in first order. When the 4% zero-order mirror was replaced with optics of higher reflectivity, the frequency selectivity of the coupled cavity decreased. With a zero-order mirror reflectivity of 10%, we could achieve SLM operation only with very careful adjustment of the cavity alignment. At a reflectivity of 25% the OPO was multimode, and at a reflectivity of 65% the OPO behaved as a linear cavity, with a bandwidth of a few nanometers.

To predict the mode spacing of our coupled cavity, we developed a model similar to that employed by Smith<sup>8</sup> to evaluate the mode spacing for a Fox-Smith cavity.<sup>7</sup> In the Michelson-mirror cavity we use a beam splitter whose transmission and reflection properties were later changed to represent the features of the diffraction grating. By considering a wave  $\exp(i2\pi\nu_0 t)$  incident from the left in Fig. 3 upon beam splitter  $M_2$ , we can find the wave returning to  $M_2$  from subsequent reflections from mirrors  $M_3$  and  $M_4$ . From this, the gain  $g$  can be calculated. The requirement that the gain must be real gives the resonance condition

$$-\frac{\tau_2^2 \rho_3}{\rho_2^2 \rho_4} \sin \frac{4\pi\nu}{c}(L_1 + L_2) = \sin \frac{4\pi\nu}{c}(L_1 + L_3), \quad (1)$$

where  $\rho_i$  and  $\tau_i$  are, respectively, the amplitude reflection and transmission coefficient of mirror  $M_i$ . The frequency of the wave, relative to  $\nu_0$ , is given by  $\nu$ ,  $c$  is the velocity of light, and  $L_i$  are the lengths of the interferometer arms, as given in Fig. 3. Following the

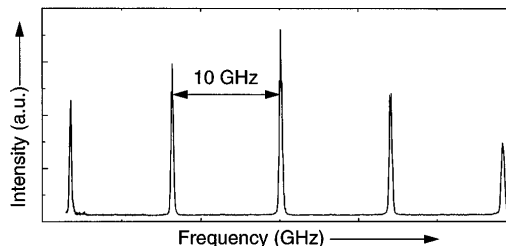


Fig. 2. Linewidth and mode analysis of the OPO signal output at 610 nm recorded with an étalon with a free spectral range of  $\sim 10$  GHz (étalon B of the pulsed laser spectrum analyzer). SLM operation is shown, for a grating angle of  $88.6^\circ$ .

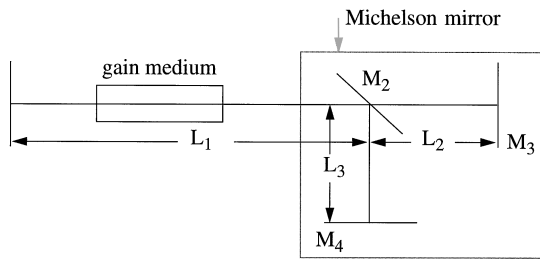


Fig. 3. Longitudinal-mode selection with a Michelson-mirror cavity containing the two coupled cavities  $M_1M_4$  (linear cavity) and  $M_2M_3$ .

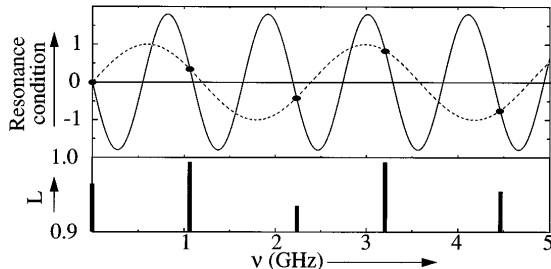


Fig. 4. Upper part: Solution of resonance condition (1) for the specific case mentioned in the text as a function of mode spacing  $\nu$ . The dashed and the solid curves correspond to the right and the left parts of resonance condition (1), respectively. The filled circles represent the solutions with positive gain. Lower part: The losses ( $L$ ) for the solutions with positive gain as a function of  $\nu$ .

treatment of Smith<sup>8</sup> we can derive the power gain ( $G = gg^*$ ), and the fractional power loss  $L$ , given by  $L = 1 - 1/G$ , is found to be

$$L = 1 - \rho_1^2[\tau_2^4 \rho_3^2 + \rho_2^4 \rho_4^2 + 2\tau_2^2 \rho_2^2 \rho_3 \rho_4 \times \cos \frac{4\pi\nu}{c}(L_2 - L_3)]. \quad (2)$$

To find the resonances of the coupled cavity, we used the values  $\rho_1 = \rho_4 = 1$ ,  $\rho_3^2 = 0.04$ ,  $L_1 = 4.5$  cm (corresponding to an optical length of 5.3 cm),  $L_2 = 8.35$  cm, and  $L_3 = 1$  cm. The grating is described as having a transmission of  $\tau_2^2 = 0.9$  (zero-order reflection) and a reflection of  $\rho_2^2 = 0.1$  (first-order diffraction). By plotting the two sides of the resonance condition as a function of  $\nu$  one can find the solutions to Eq. (1) from the intersections of the functions, as shown in the upper part of Fig. 4. Half of the solutions can be rejected, however, as having negative gain ( $g$ ), while the loss  $L$  for the remaining half (the filled circles in Fig. 4) can be calculated by Eq. (2), as depicted in the lower part of Fig. 4. Those solutions associated with the lowest loss can be expected to resonate in the cavity. Implementing the grating into the cavity implies writing the first-order reflection as  $\rho_2 = \rho_2(0)\exp\{-\ln 2[(\nu_0 - \nu_g)/\Delta\nu]^2\}$ ,<sup>10</sup> where  $\nu_g$  is the frequency that is optimally selected by the grating (and the tuning mirror) and  $\Delta\nu = c/N(\alpha)\lambda$  is the grating bandwidth with  $N(\alpha)$  the number of illuminated lines on the grating. This means that only those modes that fall within the grating bandwidth will be resonated.

Our cavity parameters differ considerably from those of the more general case, where  $\rho_1 = \rho_3 = \rho_4 = 1$  and  $\rho_2^2 = \tau_2^2 = 0.5$ . In these circumstances the solutions

of the resonance condition (1) experiencing the lowest loss all coincide, with the resonance condition being equal to zero.<sup>8</sup> All solutions in between have high losses. The mode spacing is then expressed in the general form  $c/2(L_2 - L_3)$ . Therefore lengths  $L_2$  and  $L_3$  are usually chosen to be almost equal to give a large mode spacing. In our case, however, a general form of the mode spacing cannot be given, and the largest mode spacing does not necessarily result from making  $L_2$  and  $L_3$  almost equal. Solving Eqs. (1) and (2) shows that the resonance exhibiting the lowest loss corresponds to a 2.2-GHz mode spacing, as shown in Fig. 4. Experimentally, by changing the grating angle to  $87^\circ$ , we were able to show multimode operation with a mode spacing of 2.25 GHz. By varying the lengths of the different arms of the cavity we checked that the model presented here can fully explain the changes in mode spacing observed.

In conclusion, we have demonstrated a coupled-cavity OPO design capable of SLM operation and of high external efficiencies compared with those of a conventional grazing-incidence cavity. The design includes an additional mirror with a reflectivity comparable with the first-order diffraction efficiency of the grating to form the coupled cavity. The use of this coupled-cavity OPO as a scanning device for applications in spectroscopy is currently being investigated. It requires the simultaneous adjustment of the lengths of both cavities and (for large tuning ranges) of the angle of the nonlinear crystal and the tuning mirror.

We gratefully acknowledge the support of the Netherlands Centrum voor Laser Research b.v., Urenco (Capenhurst, UK), and the British Council. L. A. W. Gloster also thanks the Engineering and Physical Science Research Council for support. A patent on this new cavity design is pending.

## References

1. V. G. Dmitriev, G. G. Gurzadyan, and D. N. Nikogosyan, in *Handbook of Nonlinear Optical Crystals*, A. E. Siegman, ed. (Springer-Verlag, New York, 1991), Vol. 64, p. 181, and references therein.
2. J. M. Boon-Engering, W. E. van der Veer, J. W. Gerritsen, and W. Hogervorst, *Opt. Lett.* **20**, 380 (1995); A. Fix, T. Schröder, R. Wallenstein, J. G. Haub, M. J. Johnson, and B. J. Orr, *J. Opt. Soc. Am. B* **10**, 1744 (1993).
3. G. Robertson, A. Henderson, and M. H. Dunn, *Appl. Phys. Lett.* **62**, 123 (1993).
4. W. R. Bosenberg and D. R. Guyer, *J. Opt. Soc. Am. B* **10**, 1716 (1993).
5. L. A. W. Gloster, I. T. McKinnie, Z. X. Jiang, T. A. King, J. M. Boon-Engering, W. E. van der Veer, and W. Hogervorst, "Narrow-band  $\beta$ -BaB<sub>2</sub>O<sub>4</sub> optical parametric oscillator in a grazing-incidence configuration," *J. Opt. Soc. Am. B* (to be published).
6. A. E. Siegman, *Lasers* (University Science, Mill Valley, Calif., 1986), pp. 524–531.
7. P. W. Smith, *Proc. IEEE* **60**, 422 (1972).
8. P. W. Smith, *IEEE J. Quantum Electron.* **QE-1**, 343 (1965).
9. J. Pinard and J. F. Young, *Opt. Commun.* **4**, 425 (1972).
10. B. Tromborg, H. Olesen, X. Pan, and S. Saito, *IEEE J. Quantum Electron.* **QE-23**, 1875 (1987).